Geomechanics and Engineering, *Vol. 19, No. 2 (2019) 153-165*
DOI: https://doi.org/10.12989/gae.2019.19.2.153

EPB tunneling in cohesionless soils: A study on Tabriz Metro settlements

Amir H. Rezaei*[1], Mojtaba Shirzehhagh[2] and Mohammad R. Baghban Golpasand[3]

[1]*Department of Civil Engineering, Azarbaijan Shahid Madani University, PO Box: 5375171379, Tabriz, Iran*
[2]*Department of Civil Engineering, Tarbiat Modares University, PO Box 14115-175, Tehran, Iran*
[3]*Department of Civil Engineering, Seraj Institute of Higher Education, PO Box 5137894797, Tabriz, Iran*

(Received July 26, 2019, Revised September 16, 2019, Accepted September 23, 2019)

Abstract. A case study of monitoring and analysis of surface settlement induced by tunneling of Tabriz metro line 2 (TML2) is presented in this paper. The TML2 single tunnel has been excavated using earth pressure balanced TBM with a cutting-wheel diameter of 9.49 m since 2015. Presented measurements of surface settlements, were collected during the construction of western part of the project (between west depot and S02 station) where the tunnel was being excavated in sand and silt, below the water table and at an average axis depth of about 16 m. Settlement readings were back-analyzed using Gaussian formula, both in longitudinal and transversal directions, in order to estimate volume loss and settlement trough width factor. In addition to settlements, face support and tail grouting pressures were monitored, providing a comprehensive description of the EPB performance. Using the gap model, volume loss prediction was carried out. Also, COB empirical method for determination of the face pressure was employed in order to compare with field monitored data. Likewise, FE simulation was used in various sections employing the code Simulia ABAQUS, to investigate the efficiency of numerical modelling for the estimating of the tunneling induced-surface settlements under such a geotechnical condition. In this regard, the main aspects of a mechanized excavation were simulated. For the studied sections, numerical simulation is not capable of reproducing the high values of in-situ-measured surface settlements, applying Mohr-Coulomb constitutive law for soil. Based on results, for the mentioned case study, the range of estimated volume loss mostly varies from 0.2% to 0.7%, having an average value of 0.45%.

Keywords: TBM-EPB; mechanized tunneling; settlements; face pressure; grouting; empirical methods; COB; FEM

1. Introduction

Urban development and growth of population have brought about a considerable increase in urban areas tunneling projects for different purposes such as urban highways, subways and railway underpasses. A major consideration in the design of tunnels in urban areas is the prediction of the ground movements and surface settlements associated with the tunneling operations (Goh and heffney 2010). To limit soil disturbance and consequent surface settlements, tunnel boring machines (TBM) are widely employed to excavate tunnels with pressurized face. TBMs generate support pressures at the tunnel face (face pressure), along the shield skin (annulus pressure) and behind the shield tail outside the lining segments (grout pressure) that play a significant role in limiting ground and buildings deformations (Mooney *et al*. 2016). Nevertheless, in the surroundings of the tunnel ineluctable ground movements could still be induced by various factors which are divided into three main groups (Lee *et al*. 1992):

- overcut due to the difference between the excavation diameter and the diameter of the shield skin (face loss)
- The conical shape of the shield (shield loss)
- Gap between the diameter of the excavation and the diameter of the lining, which is usually filled with grout injected from the shield tail (tail loss)

In this regard, lower values of mechanized tunneling-induced surface settlements could be attributable to a more precise control of face stability and tail void grout injection.

Several studies have been done to evaluate the tunneling resultant ground settlements in soil and rock masses (Mazak 2014, Fahimifar *et al*. 2015, Baghban Golpasand *et al.* 2018). Generally, these settlements are thought to be induced by ground loss, which is considered as a volume difference of theoretical and actual excavation. The gap model, which is proposed by Lee et al. (1992), estimates total ground loss as a linear sum of tail loss, face loss, and shield loss. Commonly, in order to estimate tunneling induced surface settlements, the closed-form empirical formulas are used. Those mostly predict ground settlement in terms of volume loss V_L, which is defined as ground loss per unit area of tunnel excavation, and trough width i. The parameter i indicates the distance from the ground settlement trough inflection point to the tunnel axis. The most common formula which is proposed by Peck assumes that the surface settlements resembles a Gaussian distribution in green-field condition (Fargnoli *et al.* 2013).

*Corresponding author, Assistant Professor
E-mail: Rezaei.ah@azaruniv.ac.ir
[a]Ph.D. Student
E-mail: shirzehhaghmojtaba@modares.ac.ir
[b]Ph.D.
E-mail: golpasand.mr@seraj.ac.ir

http://www.techno-press.org/?journal=gae&subpage=7
ISSN: 2005-307X (Print), 2092-6219 (Online)

The effects of adjacent buildings on surface settlements was studied by several researchers (Ding *et al.* 2017).

1.1 Tunneling induced- surface settlements

Underground excavation in urban areas associated with the ground movements engenders surface settlements. Settlement trough is increasingly important due to the existence of surface structures. Transverse settlements trough at a sufficient distance from the tunnel face, and under the green-field condition, can be well described by a Gaussian distribution curve, with the following expression (Peck 1969)

$$S_v(x) = S_{v,max}\, exp\,(-x^2/2{i_x}^2) \qquad (1)$$

where $S_{v,max}$ is the maximum surface settlement in correspondence to the tunnel center line and x is the distance from the center line. The parameter i_x is the settlements trough width parameter. For most practical purposes, i_x can be related to depth of the tunnel centerZ_0, by a linear expression (Wang *et al.* 2016, Fang *et al.* 2017)

$$i_x = KZ_0 \qquad (2)$$

where K is a trough width constant parameter that depends on the soil type and TBM excavation parameters such as tail void grouting and face support pressures (Netzel 2009). On the basis of field observations K varies from 0.2 to 0.5 for granular soils, from 0.4 to 0.6 for stiff clays and from 0.6 to 0.75 for soft clays (Mair and Taylor 1997). However, Rankin (1988) presented $K=0.25$ for sandy grounds and For Dutch projects, Netzel (2009) reported $K=0.3$ based on field data analysis.

Empirical longitudinal settlements trough was approached by cumulative Gaussian probability curve with the following expression

$$S_v(y)_{x=0} = (S_{v,max}\,/i_y\sqrt{2\pi})\int_{-\infty}^{y} exp(-y^2/2i_y^2)\,dy \qquad (3)$$

where y is longitudinal coordinate on the tunnel center line and i_y remarks the inflection point distance on the longitudinal settlements trough which is usually assumed to be equal toi_x.

1.2 Volume loss

One of the important features of ground movements caused by TBM tunneling is volume loss(V_L), defined as

$$V_L = V_S/A_t \times 100\% \qquad (4)$$

V_s is the volume of the surface transverse settlement trough per tunnel unit length and A_t is theoretical cross section of tunnel. This parameter stems from the relaxation and the convergence of the soil around TBM inward the tunnel as illustrated in Fig. 1. The volume loss causes the settlement trough at the surface and in undrained conditions; the volume of this settlement trough (V_s) is equal to (ΔV) in unit length

$$V_s = \Delta V \qquad (5)$$

Then, considering the equations (4) and (5), the volume

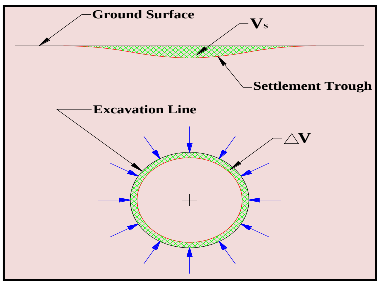

Fig. 1 Schematic illustration of Vs, At and ΔV

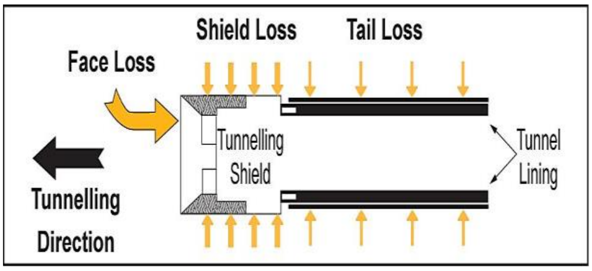

Fig. 2 The Components of Ground Loss (Loganathan 2011)

loss may be expressed as

$$V_L = 4V_s/\pi D^2 \qquad (6)$$

In many real cases V_L value is chosen on the basis of the TBM technological specifications, excavation method and previous tunneling projects experience in similar geotechnical conditions. Many preceding studies have been done around this issue and several values (or ranges) have been proposed for it based on soil types. Based on the geological and geotechnical characteristics of soil and the method of tunnel excavation, V_L can be variable between 0.2~2% (Baghban Golpasand *et al.* 2016). Netzel (2009) analyzed field data from 3 tunnels excavated in soft soil in Netherlands and determined the volume loss values for Dutch project in the range of 0.15% up to 1.5%. As reported by Mair (1996) for EPB tunneling, V_L is often as low as 0.5% in sands and in soft clays it is about 1–2%. According to the importance of variation of volume loss (V_L) on the prediction of ground settlement due to tunneling and high dependence of maximum ground settlement (S_{max}) on this parameter, it is necessary to evaluate this parameter exactly.

Loganathan (2011) stated that volume loss in mechanized tunneling have three main components including face loss, shield loss and tail loss. The total volume loss is obtained by

$$V_L = V_{Face} + V_{Shield} + V_{Tail} \qquad (7)$$

where V_{Face}, V_{Shield} and V_{Tail} are the face loss, shield loss and tail loss, respectively. Physical concept and the position of the volume loss components are shown in Fig. 2. Loganathan proposed analytical methods to determine the amount of each of the components of volume loss. The methods are associated to the empirical parameters that are obtainable using some of geotechnical properties of soil and geometrical dimensions of the shield. It should be noted that some of these parameters are dependent on the empirical values and are associated with high uncertainty. Therefore, the use of this method has been limited in any situations so another solution should be selected to specify the real value of volume loss.

However, due to the inability of empirical methods to consider the supporting actions of the TBM effect in determination of V_L, the relatively conservative V_L values is usually adopted in ground settlement control. As a result, the ground settlement is estimated conservatively, which may leads to unnecessary ground improvement as counter measures. Hence, for economic design of TBM tunneling, reasonable prediction of V_L is essential on the basis of dependable analysis of settlement. Although considerable researches has been devoted to correlate the volume loss with TBM operation parameters directly, most of them could not achieve statistically meaningful relationships, due to the extremely complicated process of TBM tunneling, (Jones, 2010). Likewise as only limited number of field monitoring data have been presented for mechanized tunneling in coarse-grained soils, limited indications are provided for proper applying of the empirical formulas parameters.

In this paper the case of the line 2 of the Tabriz metro is presented. The main purpose is to collect and interpret field monitoring data recorded during the construction of the western part of TML2 through the populated area. The tunnel having a diameter of 9.49m is being excavated in sand and silt, at a depth of about 16 m and generally below the water table. The measured settlements are back-analyzed using the Gaussian empirical predictions, in both longitudinal and transverse sections, to figure out the values of settlement trough width constant K and volume loss V_L. It provides a comprehensive description of the EPB (Earth Pressure Balance) performance under such a geotechnical condition. Besides, the reliability and validity of common methods used for the estimating tunneling-induced settlements is investigated, in comparison with TML2 monitored data. In addition, the influence of excavation parameters recorded during tunnel construction, such as tunnel face and back-filling grouting pressure, is discussed. Finally, ABAQUS 3D numerical simulation results is compared with the original and translated Gaussian distribution curve proposed by Peck (1969).

2. The line 2 of Tabriz urban railway

Tabriz (population 1,773,033) is the fifth most populated city of Iran. It is located in the north-east region of the country. Tabriz metro line 2 (TML2) with an approximate total length of 22 km and 20 stations runs from the west region to the east part of the city (Katebi *et al.* 2015). The general layout of Tabriz metro lines is shown in Fig. 3. This study is focused on the west part of line 2 between west depot (from chainage 1800) and S02 station (chainage 3800). In this part the main geological unit is Quaternary alluvium. The layers are characterized by a broad range of soil ranging from well graded gravel to some fine grained soils such as silts and clay terms. One of the main parameters for soil classification is percentage of fines (passed form No.200 sieve). Considering this parameter and other factors such as mechanical properties, cohesive (for fine-grained soils), permeability (for coarse-grained soils)

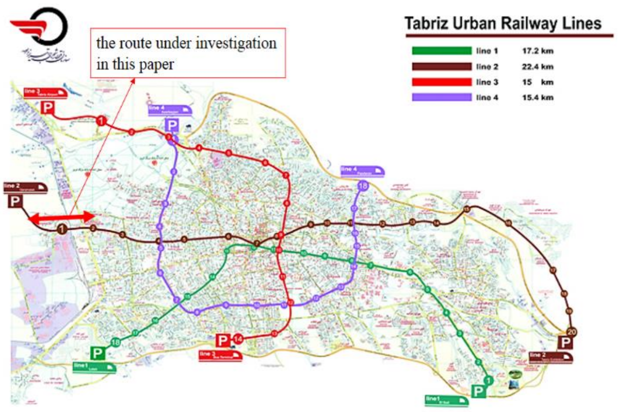

Fig. 3 Tabriz Urban Railways and the under study west part of the line 2

Table 1 Engineering geological characteristics of soil types

Engineering geological types	TG1	TG2	TG3	TG4
Soil description	Silty clay or clayey silt with a little sand	Clayey silt or silty clay with sand and gravel	Very silty clayey sand with gravel	Sandy gravel or gravely sand with silt or clay
Passing from N.200 sieve (%)	>75	50-75	25-50	<25
USCS	CL, ML, CL-ML, rarely CH	CL, ML, CL-ML	SM, SC, SC-SM, rarely GM	SM, SP, GP, SW, GW , GM

the tunnel's surrounding soil strata could be classified into 4 engineering geological types named TG1-TG4 (Table 1). The geological cross section along the tunnel route and tunnel alignment are presented in Fig. 4.

As seen in Fig. 4, tunnel passes mainly through TG-1 and TG-2 types and overburden layers contain TG-3, TG-4 and filling material. According to the project geotechnical report, ground condition could be characterized as three main strata in this region: filling material upper layer; fine grained alluvial layer and sandy alluvial (geodata.it). Table 2 summarizes the geotechnical parameters at tunnel depth. Therefore, the ground conditions would be categorized into coarse-grained soil or a combination of sand, silt and clay with negligible value of cohesion (Mohammadi *et al.* 2016).

The TML2 tunnel has been excavated using EPB-TBM with a cutting-wheel diameter of 9.49 m. The TBM shield length and thickness are 9 m and 50 mm, respectively. The shield has external diameter of 9.46 m at the face and 9.44 m at the tail. Precast concrete segments characterized by a length of 1.5 m and a thickness of 350 mm are installed just behind the shield to support the tunnel. Between the west depot and S01 station, the phreatic level varies 13-16 m, from the ground surface. In the same way, from the S01 station to the S02 station (Fig.4a), it varies over the range 14-22 m. Fig. 5 illustrates the tunnel axis depth and the phreatic level changes along the TML2 route in the mentioned part. The tunnel was constructed in shallow depth by crossing the residential area, and hence, it was required to minimize surface settlement and avoid possible damages to adjacent buildings.

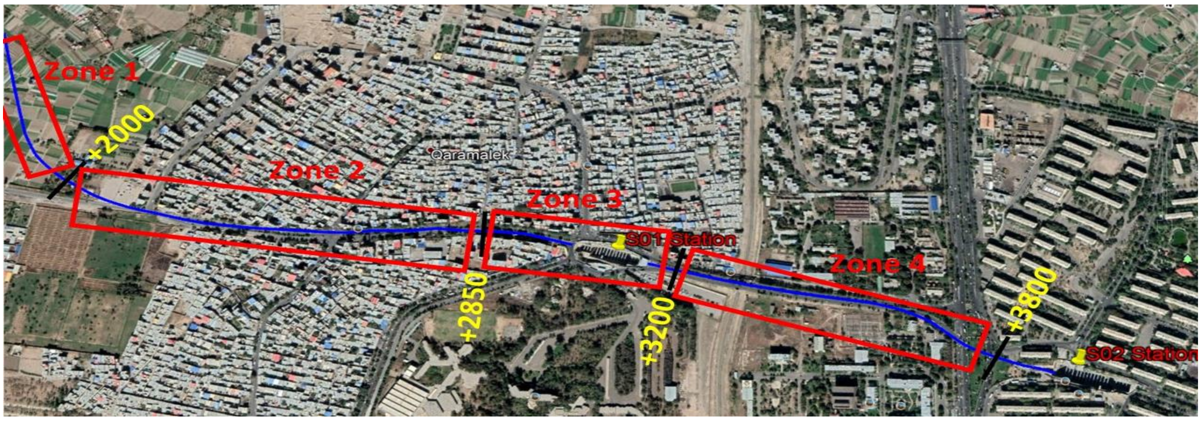

(a)

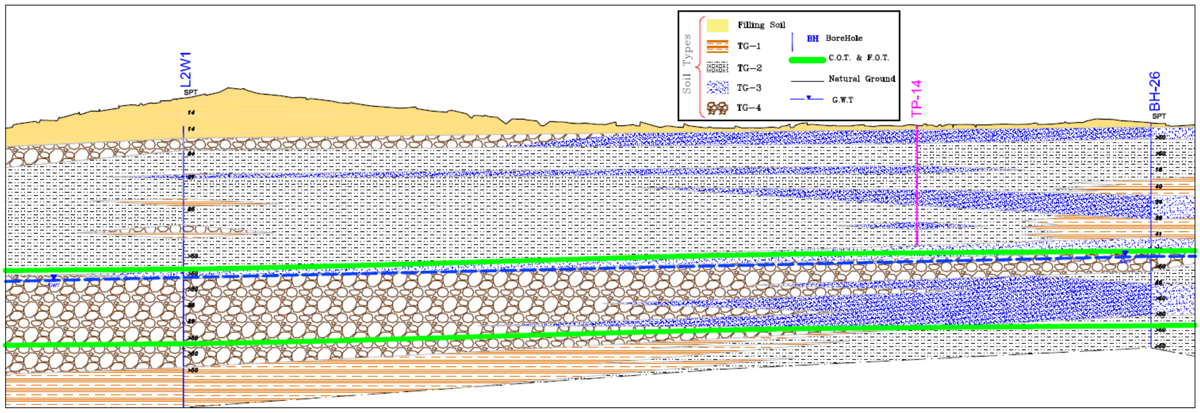

(b) Geological profile section 2+200-2+800 (zone 2)

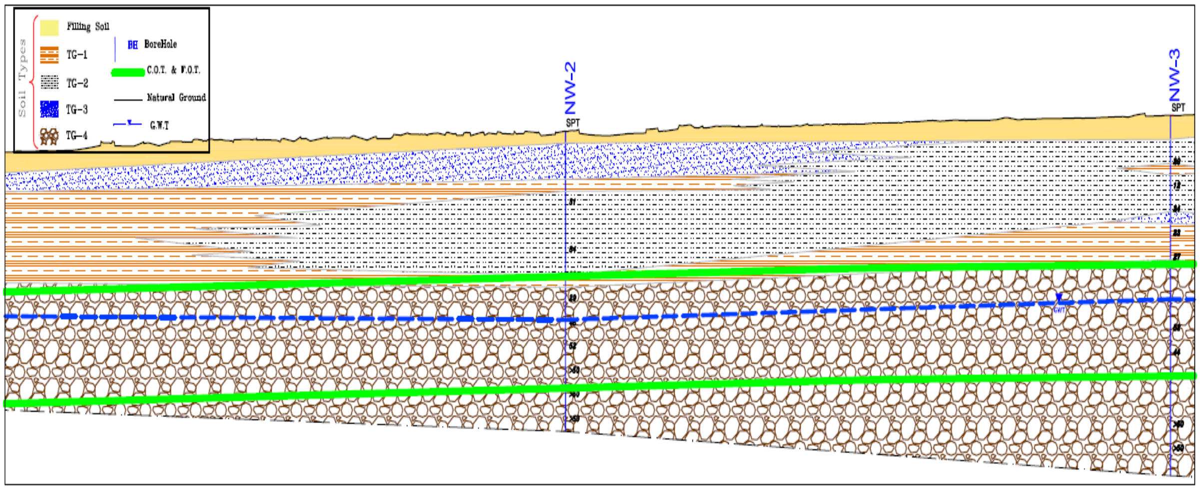

(c) Geological profile section 3+200-3+800 (zone 4)

Fig. 4 (a) Tunnel alignment along the TML2, (b) and (c) Geological profile

3. Monitoring details

This paper presents the surface settlement measurements during construction of west part of TML2. The monitoring reading them by appropriate surveying instruments, logging and primary processing. In the mentioned project, in order to monitor surface settlement, standard marker pins were used (Fig. 6). These pins were planted directly above the tunnel center line along the route, at average spacing of 10 meter. For about 2000 meters long subjected to study, 168 sections were instrumented. Considering the high number of measurement pins, only the data of 20 sections (Table 2) that were selected randomly all along the route are presented. Because most of the tunnel alignment was along the heavy traffic narrow road crossing the residential and industrial area, it was hard to measure the ground settlement out of tunnel axis and focus of this paper is on the longitudinal ground surface settlements profiles. However, in about section 2+577, some monitoring points in different horizontal distances from the tunnel axis, were surveyed. In addition to surface settlement, the values of the face pressure applied by EPB and the values of the tail void

Table 2 Geotechnical parameters of the studied region at the tunnel depth

Tunnel Chainage (*m*)	500- 2000	2000- 2850	2850- 3200	3200-3800
Zone (in Fig. 2(a))	1	2	3	4
USCS	SM	SM	SM, SC, ML	SM
$N_{spt\text{-}modified}$	>50	30-50	40-60	30-50
Dry Density (gr/cm^3)	1.70-1.75	1.65-1.70	1.63-1.75	1.65-1.75
Saturated Density (gr/cm^3)	1.85-2.05	1.75-2.00	1.91-2.09	1.85-2.00
Undrained Cohsion (Kg/cm^2)	0.15-0.25	0.10-0.20	0.20-0.30	0.10-0.20
Drained Cohesion (Kg/cm^2)	0.10-0.15	0.05-0.10	0.10-0.20	0.05-0.10
Undrained Internal friction (*deg*)	22-24	20-22	21-23	29-31
Drained Internal friction (*deg*)	30-32	28-30	27-29	31-33
Elasticity Modulus (Kg/cm^2)	500-600	400-500	400-500	400-600
Poisson's Ratio	0.32-0.34	0.30-0.32	0.36-0.38	0.33-0.35
Permeability Constant (*cm/s*)	1E-04 – 1E-05	1E-04	2.5 E-05	1E-05
Tunnel Cover (*m*)	8-12	10-13	13-18	15-23

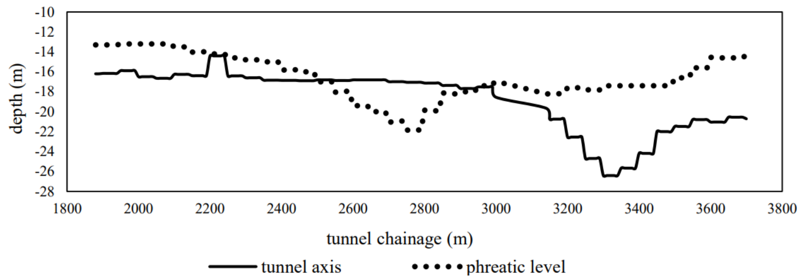

Fig. 5 Tunnel axis depth and underground water table

Fig. 6 Installation process of used marker pins for surface settlement monitoring

Table 3 Monitoring sections; numbers shows the chainage of pins

S_2235.35	S_2199.86	S_2156.44	S_1966.88
S_2559.87	S_2423.50	S_2384.57	S_2318.13
S_2970.18	S_2850.58	S_2779.80	S_2706.88
S_3485.00	S_3390.00	S_3318.00	S_3185.00
S_3272.00	S_2054.39.00	S_3699.00	S_3592.00

grouting injection pressures were continuously monitored for each ring.

4. Numerical simulation

In recent years, various aspects of mechanized tunneling has been studied applying different numerical methods

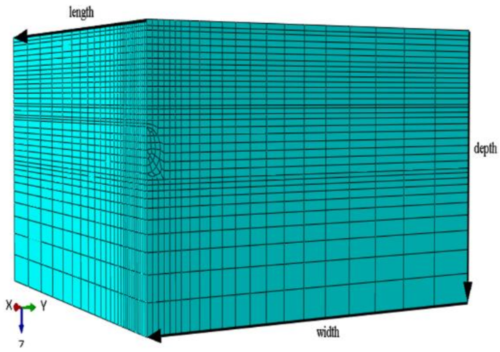

Fig. 7 The finite element model adopted for this study

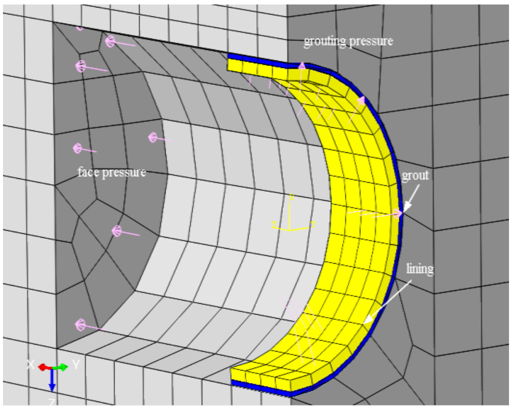

Fig. 8 3D FEM simulating of TBM tunneling

Table 4 Parameter values for the equivalent overcut layer, lining, grout and TBM shield

Parameter	υ	E	γ
unit	-	MPa	kN/m^3
Shield	0.25	210000	-
Overcut	0.20	0.10	-
Lining	0.20	25200	25
Grout (fluid)	0.47	50	18
Grout (hardened)	0.30	20	18

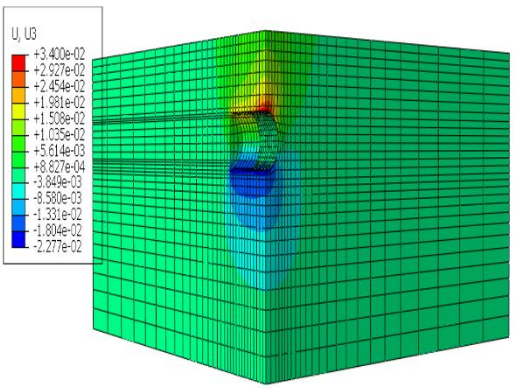

Fig. 9 Contour of FE resultant vertical displacements

(e.g., Das *et al.* 2017, Hasanpour *et al.* 2017). To examine ground surface settlements during TML2 tunneling, a 3D finite element (FE) simulation was used by the code Simulia ABAQUS. All the important components of TBM tunneling such as TBM shield, overcut, segmental lining and tail void grout (including time-dependent grout hardening) were implemented. The constitutive model assumed for the soil behavior was the linear elastic-perfectly plastic Mohr–Coulomb model (MC) with a non-associated flow rule. The mechanical behavior of the overcut layer, TBM shield, segmental lining and tail void grout was simulated based on the linear elastic constitutive model (LE).

4.1 Simulating the domain

According to previous research, many rules were published for the optimum dimensions of the domain, in order to minimize the boundary effects (Lambrughi *et al.* 2012, Katebi *et al.* 2015). In the proposed model, the values recommended by Lambrughi (2012) have been selected as the following:

- $Z_0 + 4D$, for the mesh depth
- $2(Z_0 + 4D)$, for the mesh length and width

It is a common practice in numerical simulations to use symmetry with respect to a vertical plane including the tunnel axis (Kavvadas *et al.* 2016). Hence, in the present paper, only half of the domain was simulated. The soil above the phreatic level was discretized using continuous 8-noded full-integrated C3D8 elements. The saturated soil under the water table, was simulated using pore pressure C3D8P elements. Fig. 7 shows the finite element model used for this study.

4.2 Simulating the Overcut

As it was previously described, overcut is primarily attributable to that the cutter-head diameter is larger than the shield external diameter. In this case, the difference between excavation diameter (9.49 m) and shield skin varies from 3 cm in front of shield to 5 cm at the tail, due to shield shape. The effect of this gap was considered by defining a thin layer with linear elastic continuous elements. For the sake of simplicity, the thickness of the overcut layer has been assumed to be equal to 2 cm which is the average value of the gap between the excavation boundary and the shield skin.

4.3 Simulating the TBM shield and the segmental lining

TBM shield and segmental lining were simulated using 4-noded full-integrated quadrilateral shell elements. The shield was simulated by replacing a simplified cylindrical shape with the external diameter of 9.45 m instead of its original conical shape. The weight of TBM and its Back-up train was 650 tons and 320 tons, respectively. Since the Back-up train enters the excavated tunnel, shield density was increased to consider the TBM Back-up in simulation. The external diameter of the segmental lining is 9.18 m. Mechanical properties assigned for lining was assumed to be equal to concrete.

4.4 Simulating the tail void grouting

Two component grout was injected to fill the 155 mm gap between the segmental lining extrados and the excavated diameter. In order to simulate the tail void grout, continuous 8-noded elements were used adopting a linear elastic behavior. The time-dependent hardening of grout was assigned by progressive increase of its Young's modulus, as shown in Table 4. Fig. 8 presents the considered separate components in the model.

4.5 More details about the simulation

EPB recorded face and grouting pressures were used as inputs into the numerical simulations. In this case, tail grouting annulus and face support pressure are assumed to vary linearly with elevation according to a bulk density of the muck equal to 13 KN/m^2 which could be considered as operative conditions. Grout hardening completion takes 8 hours. Since a constant advance rate of 0.75 m/h was adopted for TBM advance, the annulus grouting pressure applied to the tunnel face was eliminated after installation of 4 lining rings, at the moment when grout had been changed from fluid state to hardened condition (Kasper and Meschke 2006, Katebi *et al.* 2015). Mechanical properties of TBM components are presented in Table 4. Numerical simulations was used for Section_2199.88, 2832.76, 3185 and Section_3318. Soil stratigraphic profiles and tunneling details for these sections are shown in Tables 5-8. In this regard Fig. 9 illustrates the contour of FE analysis resultant settlements in one of the sections.

5. Results and discussion

The in-situ (real) settlements caused by the excavation of the TML2 tunnel were experimentally measured on site by leveling points installed at the ground surface. In this part of paper these settlements which have been gathered under steady state conditions at the 168 instrumented sections are presented. At each of these sections tunnel face was sufficiently far from the section, representing the settlements had not been affected by the excavation advancement. Fig. 10 Shows that the average value of the final surface settlements is only slightly more than 20 mm, in this rout, which indicates that the excavation parameters has been controlled in a good way by the operators.

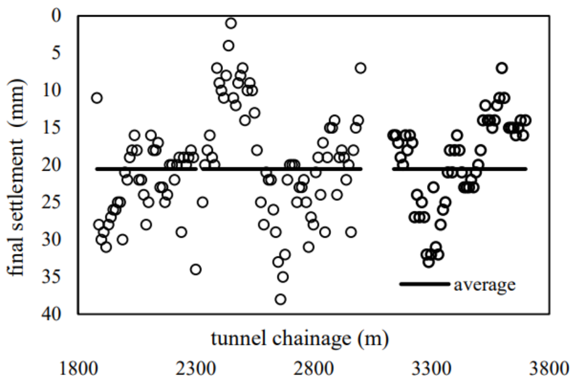

Fig. 10 Final surface settlements recorded during the tunnel advancement

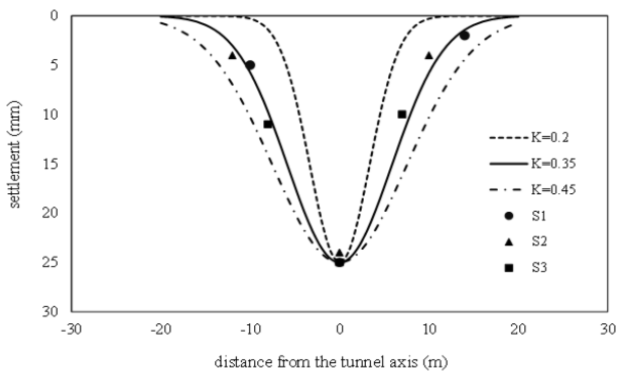

Fig. 11 interpretation of measurements by a Gaussian curve

Table 5 Section 2+199.88; stratigraphic profile

Parameter	Thickness	E	ν	φ	C	γ_d	γ_{sat}
unit	m	kgf/m^2	-	deg	kPa	kN/m^3	kN/m^3
layer1	2.00	10	0.30	22.0	10	18.00	18.00
layer2	5.98	110	0.40	21.9	13	15.60	17.80
layer3	0.90	585	0.33	35.2	4	15.50	18.30
layer4	3.46	110	0.40	24.7	17	15.80	18.50
layer5	1.42	220	0.40	32.0	5	17.50	20.30
layer6	1.10	300	0.40	23.2	37	16.50	20.30
layer7	Base	385	0.33	35.6	3	17.10	20.00

Table 6 Section 2+832.76; stratigraphic profile

Parameter	Thickness	E	ν	φ	C	γ_d	γ_{sat}
unit	m	kgf/m^2	-	deg	kPa	kN/m^3	kN/m^3
layer1	4.60	10	0.30	22.0	10	18.00	18.00
layer2	1.11	55	0.33	28.3	19	15.70	19.40
layer3	7.50	90	0.40	14.0	73	16.70	19.60
layer4	1.06	965	0.33	14.0	42	16.50	18.70
layer5	5.94	155	0.40	18.0	44	16.70	20.50
layer6	2.60	795	0.33	21.6	14	16.70	20.80
layer7	0.97	120	0.35	30.5	8	16.50	20.10
layer8	Base	795	0.33	21.6	14	16.80	21.20

Table 7 Section 3+185; stratigraphic profile

Parameter	Thickness	E	ν	φ	C	γ_d	γ_{sat}
unit	m	kgf/m^2	-	deg	kPa	kN/m^3	kN/m^3
layer1	2.33	10	0.30	22.0	10	18.00	18.00
layer2	1.05	55	0.33	28.3	19	15.70	19.40
layer3	6.96	90	0.40	22.0	27	16.00	18.00
layer4	2.86	965	0.33	14.0	7	16.50	18.70
layer5	2.67	135	0.35	8.5	57	17.00	20.10
layer6	4.13	795	0.33	21.6	14	16.70	20.80
layer7	1.30	120	0.35	27.0	12	16.50	20.10
layer8	4.89	790	0.33	32.0	7	16.00	20.40
layer9	Base	120	0.35	28.0	12	16.50	20.10

After excluding the abnormal settlement recorded at the

Table 8 Section 3+318; stratigraphic profile

Parameter	Thickness	E	ν	φ	C	γ_d	γ_{sat}
unit	m	kgf/m^2	-	deg	kPa	kN/m^3	kN/m^3
layer1	1.27	10	0.30	22.0	10	18.00	18.00
layer2	0.93	55	0.33	28.3	19	15.70	19.40
layer3	5.63	90	0.40	22.0	27	16.00	18.00
layer4	3.35	965	0.33	14.0	7	16.50	18.70
layer5	3.50	135	0.35	8.5	57	17.00	20.10
layer6	3.37	795	0.33	21.6	14	16.70	20.80
layer7	2.31	120	0.35	27.0	12	16.50	20.10
layer8	3.09	790	0.33	32.0	7	16.00	20.40
layer9	Base	120	0.35	28.0	12	16.50	20.10

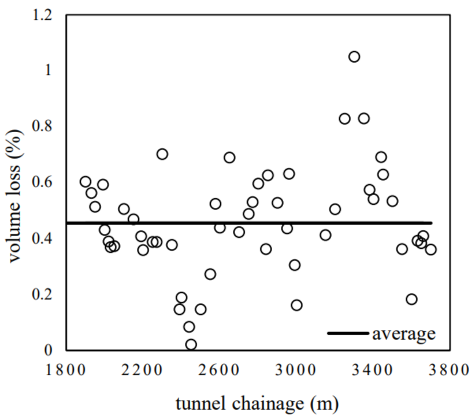

Fig. 12 Obtained volume loss values assuming the parameter K=0.35

Table 9 FE analyzed sections main data

Section	Tunnel axis depth (m)	Average applied face pressure (kPa)	Average applied grouting pressure (kPa)	Phreatic level depth (m)
2+199.88	14.415	80.00	13.50	14.20
2+832.76	17.135	70.00	115.00	19.90
3+185.00	20.745	80.00	105.00	18.20
3+318.00	26.395	125.00	128.00	17.40

sections 2+310 and 2+320 (47 and 60 mm, respectively), it is obvious that a vast majority of final surface settlements vary in the range of 10-30 mm. According to the geotechnical studies, the highest values of ground layers Young's modulus are attributable to the examined boreholes between 2+400 and 2+600, where the lowest tunneling induced-surface settlements were occurred.

In some sections at the studied area with similar geology, final settlements were measured in transverse directions. Fig. 11 presents the measurements fitted by a Gaussian curves, using K values appropriate to cohesionless soils (Mair and Taylor 1997). As shown in Fig. 11 a Gaussian empirical distribution curve, assuming K=0.35, nicely fits the monitored settlements.

The values of the V_L are obtained assuming K=0.35, on the basis of that data recorded at the sections S1, S2 and S3 are best-fitted by a Gaussian curve characterize by K=0.35 (Fig. 12). It can be observed that V_L is always lower than 0.8%, regardless of the section 3+300. The range of volume loss mostly varies from 0.2% to 0.7%, with an average value of 0.45%, in correspondence to EPB performance reported in the literature for tunneling in cohesionless soils (Baghban *et al.* 2016). Based on Minitab data analysis software results, the mean value, variance and standard deviation of V_L values are μ=0.4483, Var=0.048 and StDev=0.1624, respectively. In fact, for closed face tunneling with TBM-EPB in such a cohesionless condition like TML2, a possible value for the average V_L is equal to 0.5% (Mair 1996), which is confirmed in this study.

On the basis of the surface settlements recorded during the excavation of the TML2 tunnel, longitudinal settlements trough were obtained at 20 sections between the west depot and the station S02. Table 3 presents the position of TBM cutter-head (tunnel face) location at each section. The evolution of settlements with the excavation advancement is observed at each monitoring section in Fig. 13.

Fig. 13 indicates that the tunneling-induced settlements at the ground surface were appeared within a distance equal to the tunnel diameter, D ahead of the tunnel face and developed entirely within a distance of 40-50 m behind the tunnel face, which is equal to $4D$-$5D$. The settlements magnitude is limited to the allowed value of 25 mm, in 17 sections, demonstrating a good achievement in the excavation control during the tunneling. At the section S_2706.88, surface settlements widely exceeded 25 mm, where water table reaches its maximum depth and ground layers weighted average value of cohesion is less than 20 kPa.

Fig. 13 also shows the surface settlement directly above the tunnel face, $S_{V,face}$ was not more than 5 mm, regardless of S_2850.58. In most sections, beyond a distance of about 2D behind the tunnel face, the evolution of settlements evolution took place with a slower rate.

In mechanized tunneling, the induced longitudinal settlements over the tunnel axis can be divided into three primary components: the first part related to the TBM shield advance, the second part associated with the tail void and the last part due to clayey soils consolidation (Fargnoli *et al.* 2013). Fig. 14 shows all the recorded longitudinal surface settlements as plotted in terms of normalized settlements($S_V/S_{V,max}$).

Fig. 14 presents that only $0.38S_{V,max}$ was developed directly above the tunnel face, at most. Along the shield passage, within a distance of 10 m behind the tunnel face, 21%-40% of maximum settlement, $S_{V,max}$ was propagated. However 80% of maximum settlement was developed within a distance of 20 m behind the tunnel face, which is equal to 2D. It can be concluded that the majority of the surface settlements took place at the shield tail void, with a smaller portion developed during the shield passage. These results have good agreement with field measurements for shield tunneling in sands and silts (Nomoto *et al.* 1995) and in sand layer overlain by clay (Ata 1996), that indicates the surface settlement directly above the tunnel face generally is lower than 0.5 $S_{v,max}$.

As it was previously described, numerical simulation was used for various sections. Table 9 presents the tunneling main data in all sections. In this regard, ground stratigraphic profiles are shown in Tables 5-8.

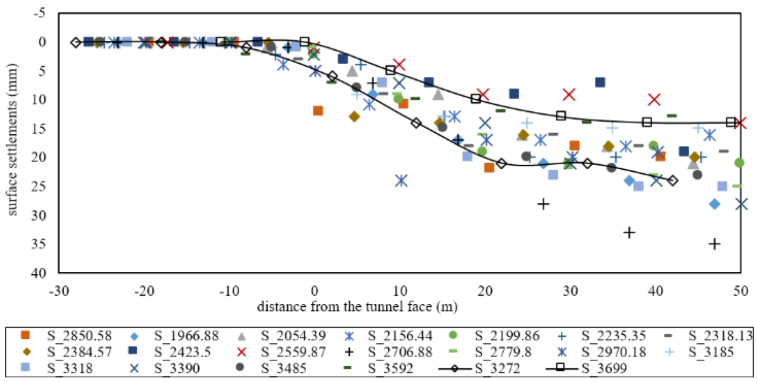

Fig. 13 Surface settlements measured above the tunnel axis as a function of the tunnel face distance

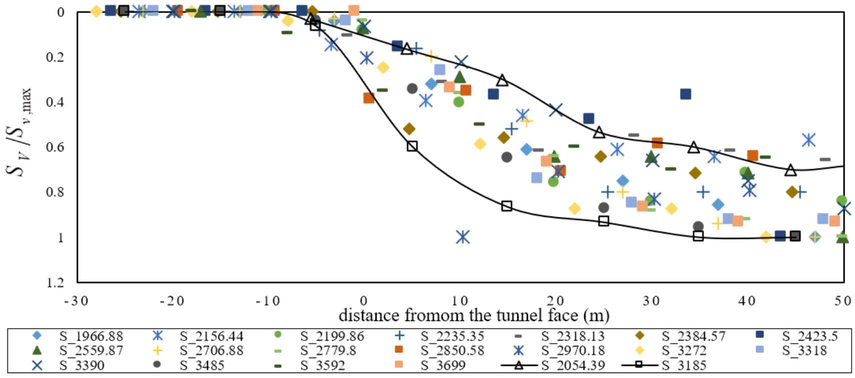

Fig. 14 Normalized surface settlements above the tunnel axis as a function of tunnel face distance

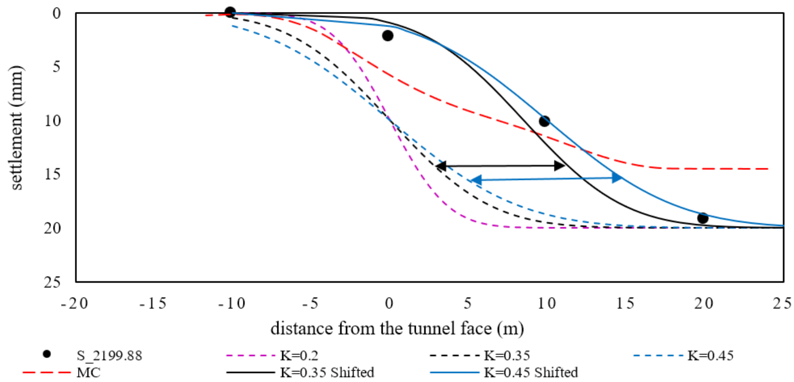

Fig. 15 Section 2+199.88; calculated and measured surface settlements in longitudinal direction

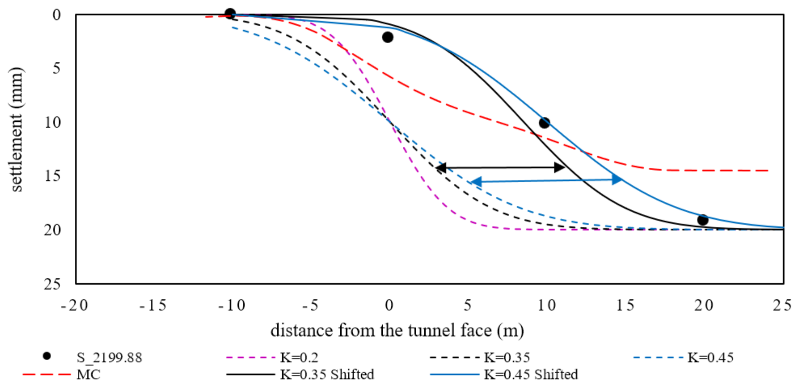

Fig. 16 Section 2+832.76; calculated and measured surface settlements in longitudinal direction

Figs. 15-18 illustrate field measurements, the associated best empirical predictions as obtained for different K values

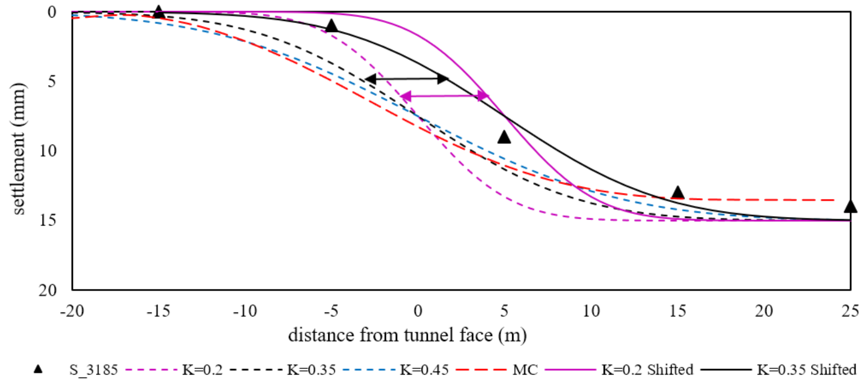

Fig. 17 Section 3+185; calculated and measured surface settlements in longitudinal direction

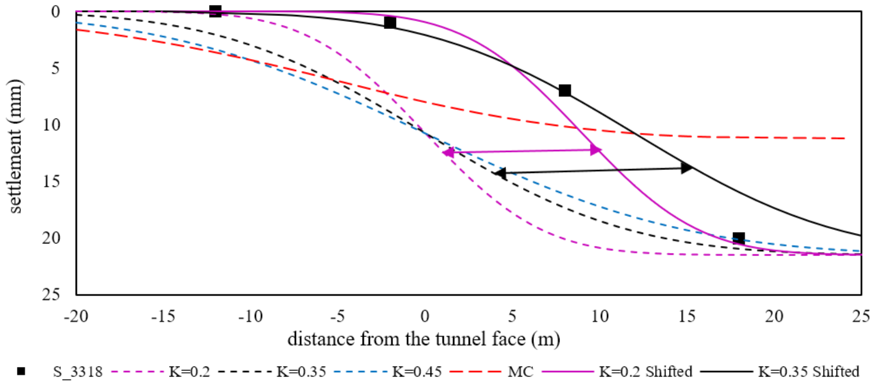

Fig. 18 Section 3+318; calculated and measured surface settlements in longitudinal direction

in the range 0.2-0.45 and FE analysis resultant surface settlements by means of Mohr-Coulomb (MC) model. It is observable from mentioned figures that the maximum settlement magnitude could be estimated accurately by Gaussian curves, but the distribution of longitudinal surface settlement doesn’t match with these curves. This induces the typically observed translation of the Gaussian curves (Fargnoli *et al.* 2013). Both translated and original Gaussian curves for the selected sections are shown in Figs. 15-18. The good consistency between the longitudinal trough and the translated Gaussian curves indicates that the main part of settlements is behind the tunnel face, as specified in the literature.

It can be seen from Figs. 15-18 that in all sections MC overestimated in calculation of settlements ahead of the tunnel face, regardless of ground conditions. However, in most sections, numerical resultant settlements were underestimated, behind the tunnel face. In general, numerical simulation by means of MC constitutive model calculated more accurately in comparison with original Gaussian empirical formula. In monitored sections, the excavation face met soils with sharply different mechanical behavior. In particular, the changes of Young's modulus is noticeably sharp, which could be considered as a problem harmfully affects FE analysis accuracy. Fig. 18 indicated that MC calculated settlements trough was completely wider than field measure, in Section_3318, where the minimum cohesion values are reported. In the same way, in Section_2832.76, MC trough was wider than field data in correspondence to the maximum phreatic level along the TML2 route.

5.1 Tunnel face support pressure

The value of sufficient pressure required to support the tunnel face stability depends on many factors such as soil properties (e.g., internal friction angle, cohesion and permeability), excavation diameter, TBM advancement rate, overburden and groundwater level. There are many variations of numerical, analytical and experimental methods in order to approach face support pressure (Guglielmetti *et al.* 2007). One of the established empirical approaches for the face support pressure determination is the method which was recommended by the Underground Construction of the Royal Dutch Institute of Engineers, known as COB. According to COB method, a sufficient face support pressure is only slightly more than the earth active pressure. The analytical methods could be subdivided into based either on the limit equilibrium (such as Anagnostou and Kovari 1996, Broere 2001) or the lower and upper bound limit analysis (e.g., Leca and Dormieux 1990, Lee 2016) methods (Zhang *et al.* 2015).

In the present paper, COB approach was employed as it is the most practical empirical method being used in engineering projects. According to the COB method, the value of the tunnel face pressure computed by the following equation, is only slightly more than the earth active pressure

$$\sigma_T = \eta_e\, k_a\, \sigma'_v + \eta_w\, \gamma_w\, H_w + 20\, kPa \tag{8}$$

where k_a is the earth active pressure coefficient, σ'_v is the effective normal stress, γ_w is water unit weight, H_w is the phreatic level and 20 kPa is a superficial surface

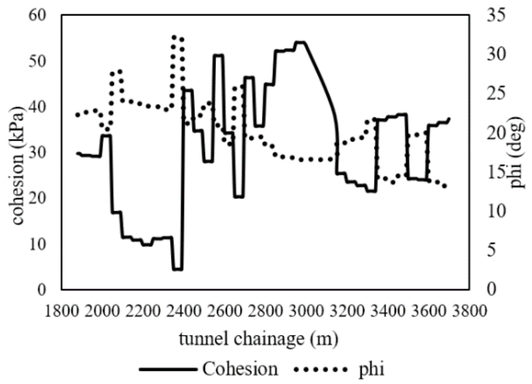

Fig. 19 Weighted average values of cohesion and internal friction angle of ground layers

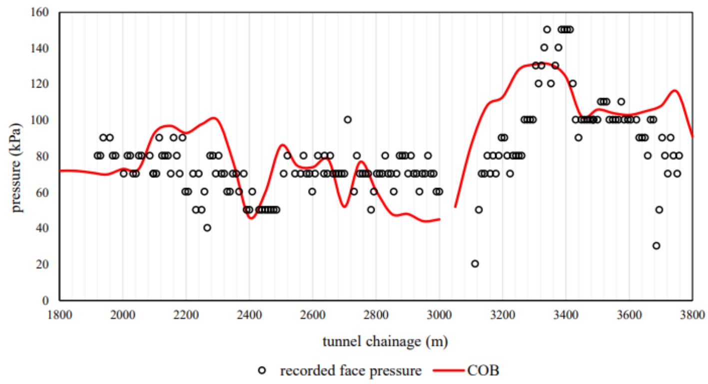

Fig. 20 Face pressure at the tunnel crown

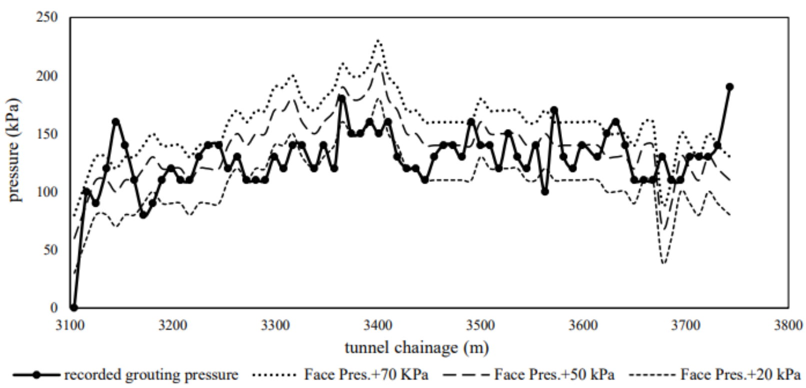

Fig. 21 Grouting injection pressure at the tunnel crown

surcharge considered as the load induced by vehicles. Likewise η_e and η_w safety factors related to earth lateral pressure and water pore pressure, respectively. The values of η_e and η_w were considered equal to 1.75 and 1.05 (Guglielmetti *et al.* 2007).

The weighted average values of cohesion, *C* and internal friction angle, φ, which are obtained on the basis of ground layers conditions, to be used in COB face pressure empirical formula are shown in Fig. 19. The figure gives an indication of the range of the changes in soil mechanical properties, along the studied corridor. It can be observed that cohesion in ground layers from section 2+300 to section 2+400 is close to zero, where surface settlements have exceptionally considerable values.

The accuracy of the employed method for determination of the face pressure is a key ingredient in TBM tunneling.

In order to assessment, Fig. 20 depicts the monitored face pressure applied in tunneling process and the values which are obtained from the COB method, for the tunnel face support pressure, at the tunnel crown. It can be observed that COB is in a good agreement with monitored pressures, which confirms the empirical method accuracy. Applied face pressures are mostly less than COB output values. It means that tunnel stability is ensured when using COB in soil with cohesion close to zero (cohesionless soil). As ground cohesion increases in the region from section 2+800 to section 3+000, COB method underestimate the required values. The results shows that during the excavation process, face support pressures was applied in a way just to limit the surface settlements value within the allowed range.

Grouting pressure for the back-filling of the concrete lining, plays an important role in surface settlements contribution. The applied grouting pressure during the TML2 boring process from station S01 to station S02, are presented in Fig. 21. It can be observed recorded values for grouting pressure are more than the applied face pressure. The difference between tail grouting and face support pressures varies from 20 *kPa* to 70 *kPa*. In general the value of grout pressure is considered to be 50 *kPa* more than face support pressure in projects.

The Fig. 21 indicates that around the section 3+300, grouting pressure has been just about 20 *kPa* more than applied face pressure, where the highest values of volume loss are recorded. However, from S01 to S02, the lowest values for the volume loss are obtained around the section 3+600, where grouting pressure has been about 50 *kPa* to 70 *kPa* more than face support pressures. Hence, a possible direct correlation between grouting pressure and volume loss associated with tunneling-induced final settlement could be observed.

6. Conclusions

In this paper, a case study of volume loss estimation for the EPB TBM tunneling case was carried out on the basis of field monitoring. Measurements of settlements recorded during the excavation of west part of Tabriz metro line 2 tunnel were analyzed. Typical values of maximum surface settlement were gathered for 168 monitoring section, represent a large database to infer the performance of EPB tunneling for such a geotechnical condition. Longitudinal settlements trough were obtained at the 20 section along the route. Also, volume loss associated with the final surface settlements were computed. Beside the Surface settlements, applied face support and tail void grouting pressures recorded during the excavation process were analyzed using empirical and numerical methods. In addition, FE analysis was implemented using the code Simulia ABAQUS for 3D simulation of TML2 mechanized tunneling and longitudinal troughs were achieved in various monitored sections. The main results are as follows:

• The settlements in transverse direction were well-fitted by a Gaussian empirical formula assuming the parameter $K=0.35$. However, settlements in longitudinal direction were overestimated by original Gaussian formula, regardless of the parameter K values reported for cohesionless soil in the literature. It seems that a translated Gaussian curves have better match the evolution of settlements during tunnel excavation process.

• In the case of the EPB TBM, a larger portion of tunneling induced surface settlements were related to the void grouting, while negligible settlement was measured in face excavation. It was observed just about 40% of maximum settlement were propagated within the shield passage, in most of the route.

• Recorded face pressures data were well-fitted with the

• COB method obtained results. The low magnitude of measured surface settlement above the tunnel face, indicates the appropriate face support during the tunnel construction.

• Based on monitored results, the range of volume loss mostly varies from 0.2% to 0.7%, with an average value of 0.45%. The maximum volume loss values are associated with the regions where applied face support and tail grouting pressures were less than the required values computed on the basis of empirical COB method.

• FE analysis by means of Mohr-Coulomb constitutive model for the soil, calculated the maximum surface settlements less than recorded measurements. In the studied sections, the Mohr–Coulomb models is not capable of reproducing the high values of the surface settlements measured in situ. Numerical modelling resultant longitudinal settlements trough was wider than field recorded data, in sections with maximum overburden and phreatic level. It was obvious that mixed face condition harmfully affected the numerical simulations.

Acknowledgments

This work was carried out in cooperation with Tabriz Urban Railway Organization (TURO). Special thanks to the TML2 CEO for providing the monitoring data.

References

Ata, A.A. (1996), "Ground settlements induced by slurry shield tunnelling in stratified soils", *Proceedings of the International Conference on North American Tunnelling'96*, Washington, D.C., U.S.A., April.

Baghban Golpasand, M.R., Do, N.A., Dias, D. and Nikudel, M.R. (2018), "Effect of the lateral earth pressure coefficient on settlements during mechanized tunneling", *Geomech. Eng.*, **16**(6), 643-654. https://doi.org/10.12989/gae.2018.16.6.643.

Baghban Golpasand, M.R., Nikudel, M.R. and Uromeihy, A. (2016), "Specifying the real value of volume loss (V_L) and its effect on ground settlement due to excavation of Abuzar tunnel, Tehran", *Bull. Eng. Geol. Environ.*, **75**(2), 485-501, https://doi.org/10.1007/s10064-015-0788-8.

Das, R., Singh, P.K., Kainthola, A., Panthee, S. and Singh, T.N. (2017), "Numerical analysis of surface subsidence in asymmetric parallel highway tunnels", *J. Rock Mech. Geotech. Eng.*, **9**(1), 170-179. https://doi.org/10.1016/j.jrmge.2016.11.009.

Ding, Z., Wei, X.J. and Wei, G. (2017), "Prediction methods on tunnel-excavation induced surface settlement around adjacent building", *Geomech. Eng.*, **12**(2), 185-195. http://doi.org/10.12989/gae.2017.12.2.185

Fahimifar, A., Ghadami, H. and Ahmadvand, M. (2015), "The ground response curve of underwater tunnels, excavated in a strain-softening rock mass", *Geomech. Eng.*, **8**(3), 323-359. http://dx.doi.org/10.12989/gae.2015.8.3.323

Fang, Y., He, C., Nazem, A., Yao, Z. and Grasmick, J. (2017), "Surface settlement prediction for EPB shield tunneling in sandy ground", *KSCE J. Civ. Eng.*, **21**(7), 2908-2918. https://doi.org/10.1007/s12205-017-0989-8.

Fargnoli, V., Boldini, D. and Amorosi, A. (2013), "TBM tunnelling-induced settlements in coarse-grained soils: The case study of the new Milan underground line 5", *Tunn. Undergr. Sp. Technol.*, **38**, 336-347, https://doi.org/10.1016/j.tust.2013.07.015.

Goh, A.T.C and Hefney, A.M. (2010), "Reliability assessment of EPB tunnel-related settlement", *Geomech. Eng.*, **2**(1), 57-69. http://dx.doi.org/10.12989/gae.2010.2.1.057.

Guglielmetti, V., Grasso, P., Mahtab, A. and Xu, S. (2007), *Mechanized Tunnelling in Urban Areas: Design Methodology*

and Construction Control, Taylor & Francis Group, London, U.K.
Hasanpour, R., Schmitt, J., Ozcelik, Y. and Rostami, J. (2017), "Examining the effect of adverse geological conditions on jamming of a single shielded TBM in Uluabat tunnel using numerical modeling", *J. Rock Mech. Geotech. Eng.*, **9**(6), 1112-1122. https://doi.org/10.1016/j.jrmge.2017.05.010.
Jones, B.D. (2010), "Low-volume-loss tunnelling for London ring main extension", *Proc. Inst. Civ. Eng. Geotech. Eng.*, **163**(3), 167-185, https://doi.org/10.1680/geng.2010.163.3.167.
Kasper, T. and Meschke, G. (2006), "On the influence of face pressure, grouting pressure and TBM design in soft ground tunneling", *Tunn. Undergr. Sp. Technol.*, **21**(2), 160-171, https://doi.org/10.1016/j.tust.2005.06.006.
Katebi, H., Rezaei, A.H., Hajialilue-Bonab, M. and Tarifard, A. (2015), "Assessment the influence of ground stratification, tunnel and surface buildings specification on shield tunnel lining loads (by FEM)", *Tunn. Undergr. Sp. Technol.*, **49**, 67-78, https://doi.org/10.1016/j.tust.2015.04.004.
Kavvadas, M., Litsas, D., Vazaios, I. and Fortsakis., P. (2017), "Development of a 3D finite element model for shield EPB tunneling", *Tunn. Undergr. Sp. Technol.*, **65**, 22-34, https://doi.org/10.1016/j.tust.2017.02.001.
Lambrughi, A., Rodriguez, L.M. and Castellanza, R. (2012), "Development and Verification of a 3D numerical model for TBM-EPB mechanized excavation", *Comput. Geotech.*, **40**, 97-113. https://doi.org/10.1016/j.compgeo.2011.10.004.
Lee, K.M., Rowe, R.K. and Lo, K.Y. (1992), "Subsidence owing to tunnelling. I. Estimating the gap parameter", *Can. Geotech. J.*, **29**(6), 929-940, https://doi.org/10.1139/t92-104.
Loganathan, N. (2011), *An Innovative Method for Assessing Tunnelling-Induced Risks to Adjacent Structures*, Parsons Brinckerhoff, Inc., New York, U.S.A.
Mair, R.J. (1996), "Settlement effects of bored tunnels", *Proceedings of the International Symposium on Geotechnical Aspects of Underground Construction in Soft Ground*, London, U.K., April.
Mair, R.J. and Taylor, R.N. (1997), "Theme lecture: Bored tunnelling in the urban environment", *Proceedings of the 14th International Conference on Soil Mechanics and Foundations Engineering*, Hamburg, Germany.
Mazek, S.A. (2014), "Evaluation of surface displacement equation due to tunnelling in cohesionless soil", *Geomech. Eng.*, **7**(1), 55-73. http://dx.doi.org/10.12989/gae.2014.7.1.055
Mohammadi, S.D., Firuzi, M. and Asghari Kaljahi, E. (2016), "Geological-geotechnical risk in the use of EPB-TBM, case study: Tabriz Metro, Iran", *Bull. Eng. Geol. Environ.*, **75**(4), 1571-1583, https://doi.org/10.1007/s10064-015-0797-7.
Mooney, M.A., Grasmick, J., Kenneally, B. and Fang, Y. (2016), "The role of slurry TBM parameters on ground deformation: Field results and computational modelling", *Tunn. Undergr. Sp. Technol.*, **57**, 257-264. https://doi.org/10.1016/j.tust.2016.01.007.
Netzel, H. (2009), "Building response due to ground movements", Ph.D. Thesis, Delft University of Technology, Delft, The Netherlands.
Nomoto, T., Mori, H. and Matsumoto, M. (1995), "Overview on ground movements during shield tunnelling–a survey on Japanese shield tunnelling", *Proceedings of the International Symposium on Geotechnical Aspects of Underground Construction in Soft Ground*.
Peck, R.B. (1969), "Deep excavation and tunnelling in soft grounds", *Proceedings of the 7th International Conference on Soil Mechanics and Foundation Engineering*, Mexico City, Mexico.
Rankin, W.J. (1988), "Ground movements resulting from urban tunnelling: predictions and effects", *Proceedings of the Conference on Engineering Geology of Underground Movements*, Nottingham, U.K., September.
Terzaghi, K. and Peck, R. (1967), "Settlement of point bearing pile foundation", *Soil Mech. Eng. Practice*.
Wang, F., Miao, L., Yang, X., Du, Y.J. and Liang, F.Y. (2016), "The volume of settlement trough change with depth caused by tunneling in sands", *KSCE J. Civ. Eng.*, **20**(7), 2719-2724. https://doi.org/10.1007/s12205-016-0250-x.
Zhang, C., Han, K. and Zhang, D. (2015), "Face stability analysis of shallow circular tunnels in cohesive-frictional soils", *Tunn. Undergr. Sp. Technol.*, **50**, 345-357. https://doi.org/10.1016/j.tust.2015.08.007.
Zhao, K., Janutolo, M. and Barla, G. (2012), "A completely 3D model for the simulation of mechanized tunnel excavation", *Rock Mech. Rock Eng.*, **45**(4), 475-497. https://doi.org/10.1007/s00603-012-0224-3.
<http://www.geodata.it/en/paesi/iran/37-metro/iran/34-tabriz-metro-line-2-iran>.

IC